Check for updates

Treatment of textile effluents by chloride-intercalated Zn-, Mg- and Ni-Al layered double hydroxides

F. Z. Mahjoubi, A. Khalidi, O. Cherkaoui, R. Elmoubarki, M. Abdennouri and N. Barka

ABSTRACT

This work involved the preparation, characterization and dyes removal ability of Zn-Al, Mg-Al and Ni-Al layered double hydroxide (LDH) minerals intercalated by chloride ions. The materials were synthetized by the co-precipitation method. X-ray diffraction, Fourier transform infrared, thermogravimetric-differential thermal analysis and transmission electron microscopy characterization exhibited a typical hydrotalcite structure for all the samples. Adsorption experiments for methyl orange were performed in terms of solution pH, contact time and initial dye concentration. Experimental results indicate that the capacity of dye uptake augmented rapidly within the first 60 min and then stayed practically the same regardless of the concentration. Maximum adsorption occurred with acidic pH medium. Kinetic data were studied using pseudo-first-order and pseudo-second-order kinetic models. Suitable correlation was acquired with the pseudo-second-order kinetic model. Equilibrium data were fitted to Langmuir and Freundlich isotherm models. The maximum Langmuir monolayer adsorption capacities were 2,758, 1,622 and 800 mg/g, respectively, for Zn-Al-Cl, Mg-Al-Cl and Ni-Al-Cl. The materials were later examined for the elimination of color and chemical oxygen demand (COD) from a real textile effluent wastewater. The results indicated that the suitable conditions for color and COD removal were acquired at pH of 5. The maximum COD removal efficiency from the effluent was noted as 92.84% for Zn-Al-Cl LDH.

Key words | chemical oxygen demand, dye removal, layered double hydroxides, textile effluent

F. Z. Mahjoubi
A. Khalidi
Université Hassan II de Casablanca, Faculté des Sciences et Techniques, Laboratoire de Chimie Physique et de Chimie Bioorganique,
BP 146,
Mohammedia,
Morocco

F. Z. Mahjoubi
R. Elmoubarki
M. Abdennouri
N. Barka (corresponding author)
Univ. Hassan 1, Laboratoire des Sciences des Matériaux, des Milieux et de la Modélisation (LS3M),
BP.145,
Khouribga 25000,
Morocco
E-mail: *barkanoureddine@yahoo.fr*

O. Cherkaoui
Higher School of Textile and Clothing Industries, Laboratory REMTEX,
Casablanca,
Morocco

INTRODUCTION

Industries such as textiles, leather, plastics, paper-making, food, rubber and cosmetics use different forms of dyestuffs, which are also present in the effluents unloaded from these industries. Annually, approximately 7×10^5 tons of dyes are produced and approximately 7×10^4 tons/year are discarded in wastewaters (Crini 2006; Gupta & Suhas 2009; Shen *et al.* 2009; Rafatullaha *et al.* 2010). The elimination of color from wastewater is a great environmental problem. Among the various methods for dyes removal such as physical, chemical, biological, electrochemical oxidation and adsorption methods, the adsorption method is one of the most operational (Zhu *et al.* 2007; Demirbas 2009; Dotto & Pinto 2011; Saleh & Gupta 2012). It is an effective physico-chemical wastewater treatment process which causes passive separation of adsorbate from an aqueous solution phase onto a solid phase.

Many industries currently use activated carbon to remove dyes from wastewater (Santhy & Selvapathy 2006). However, the high cost of activated carbon diminishes its comprehensive use. In recent years, search for the creation of new low-cost adsorbents, such as clay minerals (Elmoubarki *et al.* 2015), phosphate (Barka *et al.* 2009) and natural biosorbents (Tounsadi *et al.* 2016) has grown. However, these materials generally possess low adsorption capacities and hence, a large adsorbent

This is an Open Access article distributed under the terms of the Creative Commons Attribution Licence (CC BY 4.0), which permits copying, adaptation and redistribution, provided the original work is properly cited (http://creativecommons.org/licenses/by/4.0/).

doi: 10.2166/wrd.2016.041

Downloaded from http://iwaponline.com/jwrd/article-pdf/7/3/307/376152/jwrd0070307.pdf
by guest

dosage is needed to eliminate a feeble dye concentration of the discharges. In order to decrease the cost of wastewater treatment, tests have been invented to find other relatively lower-cost adsorbents, which have higher adsorption ability.

Some innovative materials have attracted significant attention in effective and suitable purification techniques over the last few decades (Dawood & Sen 2012). Layered double hydroxides (LDHs), recognized as anionic clay, have become a great kind of adsorbent for the purification and treatment of wastewater. LDHs have the structural formula $[M^{II}_{1-x}M^{III}x(OH)_2]^{x+}[(A^{n-})_{x/n}.mH_2O]^{x+}$, where M^{2+} and M^{3+} can be any divalent and trivalent cations in the octahedral positions within the hydroxide layers: $M^{2+} = Mg^{2+}$, Zn^{2+}, Ni^{2+}, etc. and the metal ratio $x = M^{3+}/(M^{2+} + M^{3+})$ variable ($0.2 < x < 0.33$) (Cavani *et al.* 1991).

Their structure consists of positively charged brucite-like layers, $[M^{2+}_{1-x}M^{3+}_x(OH)_2]^{x+}$, alternating with negatively charged interlayers containing anions and water molecules $[A^{n-}_{x/n}\cdot mH_2O]^{x-}$ (Lopez-Salinas & Ono 1993; Carlino 1997; Whilton *et al.* 1997; Li *et al.* 2005).

The objective and target of this work is the preparation, characterization and usage of three LDHs with different divalent metal as precursors for the adsorption of a model of anionic dyes from aqueous solution and the use of them for color and chemical oxygen demand (COD) removal from effluents produced by a textile industry. The samples were characterized by X-ray diffraction (XRD), infrared (IR) spectroscopy, transmission electron microscopy (TEM) and simultaneous thermogravimetric-differential thermal analysis (TGA-DTA). The influence of solution pH, contact time and initial dye concentration were studied in batch mode. Kinetic and equilibrium parameters were explored to interpret the adsorption mechanism. To verify the efficacy of the adsorbents for the purification of textile effluents, adsorption tests were carried out with effluent discharged from a dyeing mill. The effects of different parameters on the removal of color and COD by these precursors such as solution pH and adsorbent dose were studied in detail.

MATERIALS AND METHODS

Materials

All the chemicals used in this study were of analytical grade. $Zn(NO_3)_2.6H_2O$ (>98% purity), $Ni(NO_3)_2.6H_2O$ (100% purity), $Mg(NO_3)_2.6H_2O$ (97% purity), $Al(NO_3)_3.9H_2O$ (>98% purity), NaCl and methyl orange (MO) were purchased from Sigma–Aldrich (Germany). NaOH was purchased from Merck (Germany) and HNO_3 used from Scharlau (Spain). The real dyeing effluent was obtained from a cotton and polyester textile company named ITEX, in Casablanca, Morocco.

Preparation of LDHs

Mg–Al, Zn–Al and Ni–Al LDHs containing chloride were prepared by the co-precipitation method at controlled pH. One hundred millilitres of a solution containing 0.75 M of the desirable divalent metal ion nitrate (Mg, Zn or Ni) and 0.25 M of aluminum nitrate was added drop wise to 100 ml of a solution containing NaOH (2 M) and NaCl (0.2 M), under vigorous stirring at pH 10 for 2 h. The resultant slurries were treated hydrothermally at 80 °C for 24 h, washed repeatedly with decarbonated water and dried at 60 °C for 12 h. These samples are hereafter referred to as Zn-Al-Cl, Mg-Al-Cl and Ni-Al-Cl.

Characterization

Powder XRD patterns were recorded from $2\theta = 5$ to 70° using a Bruker-axs D2-phaser advance diffractometer operating at 30 kV and 10 mA with Cu Kα1 and Kα2 radiations. The crystalline phases in the solids prepared were identified by comparison with the Joint Committee on Powder Diffraction Standards files (38-0487, 41-1428 and 54-1030, respectively, for Zn-Al-Cl, Mg-Al-Cl and Ni-Al-Cl). Fourier transform infrared (FTIR) spectra were treated using FTIR spectrophotometer of Nicolet Avatar 330. Samples were added to KBr at a mass ratio of 1:100 and finely powdered to make pellets. The spectra were recorded with 2 cm^{-1} resolution in the interval of 4,000–400 cm^{-1}. TEM images were obtained on a TEM TECNAI G2/FEI instrument, at accelerating voltage of 120 kV. Simultaneous TGA-DTA curves were recorded on a SETARAM (SENSYSevo) instrument under an argon atmosphere in the temperature range of 30–700 °C at a heating rate of 10 °C/min. The point of zero charge (pH_{PZC}) was given by the pH drift process according to the method suggested by Noh & Schwarz (1989). The pH of NaCl

Downloaded from http://iwaponline.com/jwrd/article-pdf/7/3/307/376152/jwrd0070307.pdf
by guest

aqueous solution (50 mL at 0.01 mol/L) was adjusted to initial values from 2.0 to 12.0 by addition of HNO_3 (0.1 N) and/or NaOH (0.1 N). Then, 0.05 g of each LDH was added to the solution and stirred for 6 h. The final pH was given and designed against the initial pH. The pH_{PZC} was observed at the point for which pHfinal = pHinitial.

Retention experiments

Study of MO adsorption

Synthetic dye solution at 1 g/L was prepared by dissolving a suitable quantity of MO in distilled water and subsequently concentrations were acquired by dilution. Adsorption experiments were executed in a series of 250 mL beakers holding the desired weight (20 mg) of each LDH and 250 mL of the MO solution at the appropriate concentration. These experiments were carried out with agitation speed of 500 rpm and varying the solution pH from 2 to 12, the contact time from 5 to 360 min and the initial MO concentration from 20 to 1,000 mg/L. The solution pH was adjusted to a fixed value by addition of HNO_3 (1N) or NaOH (1N) and was determined using a SensION+ PH31 pH meter. After each adsorption test, the solid phase was isolated from the liquid solution by centrifugation at 3,000 rpm for 15 min. The rest concentrations of MO were measured by UV-Vis characteristics at maximum absorption wavelength (λ_{max} = 465 nm) with use of a TOMOS V-1100 UV-Vis spectrophotometer.

The adsorbed quantity was determined using the following equation (Vanderborght & Van Grieken 1977):

$$q = (C_0 - C) \cdot \frac{V}{m} \quad (1)$$

where q (mg/g) is the adsorbed amount, C_0 (mg/L) is the initial dye concentration, C (mg/L) is the dye concentration at a time t, V (L) is the volume of solution and m (g) is the mass of adsorbent.

Treatment of textile effluent

Textile wastewater (TWW) samples at the factory's ejected point were selected from a cotton and polyester textile effluent mill ITEX, Casablanca, Morocco. The sample was kept at temperature $\leq 5\ ^{\circ}C$ in order to avoid any change in its physico-chemical properties before utilization. Treatment tests were performed in a series of 50 mL beakers containing the appropriate dose of each LDH ranging between 0.5 and 5.0 g/L and 20 mL of the effluent at a speed of 500 rpm for 8 h. The influence of pH was investigated by varying the pH from 2 to 10. Color removal from TWW was determined from the change in UV-Vis spectrum in the range of (200–700 nm) employing a BIOCHROM BIBRA Light spectrophotometer. COD was measured by the potassium dichromate oxidation technique (American Public Health Association 1998). The COD reduction (%) was calculated using the following equation:

$$COD \text{ removal } (\%) = \frac{COD_0 - COD}{COD_0} * 100 \quad (2)$$

where COD_0 is the initial COD concentration (mg/L), and COD is the COD concentration after treatment (mg/L).

RESULTS AND DISCUSSION

Characterization

XRD analysis

The XRD patterns of the three LDHs are displayed in Figure 1. As observed from the XRD patterns, the

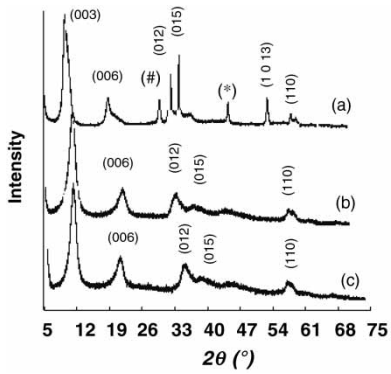

Figure 1 | XRD patterns of (a) Zn-Al-Cl, (b) Mg-Al-Cl and (c) Ni-Al-Cl, (*) $Zn(OH)_2$ and (#) $Al(OH)_3$.

Downloaded from http://iwaponline.com/jwrd/article-pdf/7/3/307/376152/jwrd0070307.pdf
by guest

hydrotalcite type phase was identified in all prepared samples (Cavani *et al.* 1991). More intensive and symmetric reflections of the (003) and (006) planes at low 2θ values (11–23°) and broad asymmetric reflections of (110) at higher 2θ values (60–62°) can be detected. The decrease in the intensity for the (110) plane in the order Zn-Al-Cl > Mg-Al-Cl > Ni-Al-Cl indicates a decrease in crystallinity. The XRD pattern of Zn-Al-Cl also showed $Zn(OH)_2$ and $Al(OH)_3$ phases impurities, which can be determined by comparison of their characteristic reflection pattern to a reference library of samples. These phases in the sample may be the consequence of poor control of the pH during the synthesis.

The lattice parameter a corresponds to an average cation–cation distance determined from the (110) reflection $a = 2d_{110}$, while the c parameter corresponds to three times the distance of (003) reflection thickness $c = 3d_{003}$. The d parameter represents the thickness of a single layer and relates to the size and orientation of the charge balancing interlayer anions, in our case, the chloride anions.

The obtained parameters are presented in Table 1. The result demonstrates that the a parameter was influenced by the cation ionic radii Zn^{2+} (0.74 Å) > Mg^{2+} (0.72 Å) > Ni^{2+} (0.69 Å) (Shannon 1976). Meanwhile, the lattice c parameter depends mostly on the size and intercalation amount of interlayer anions and on the charge density to a lesser degree. Furthermore, the important value of interlayer distance in Zn-Al LDHs may indicate the formation of an anionic bilayer.

TGA-DTA analysis

TGA-DTA curves of the LDH samples are presented in Figure 2. The curves reveal the presence of three decomposition stages. The first stage at (50–150°C) with different weight losses of 3.19, 5.47 and 8.3% for Zn-Al-Cl, Mg-Al-Cl and Ni-Al-Cl, respectively, related to the volatilization of the physically adsorbed water molecules. The other interlamellar water in the structure was eliminated up to 250°C with weight losses of approximately 7.01, 5.37 and 4.01% for Zn-Al-Cl, Mg-Al-Cl and Ni-Al-Cl, respectively.

Table 1 | Calculated unit cell parameters of the LDHs

Sample	Unit cell parameters (Å)		Interlayer distance (Å)
	c	*a*	*d*
Zn-Al-Cl	25.84	3.07	8.61
Mg-Al-Cl	23.64	3.03	7.88
Ni-Al-Cl	23.34	3.01	7.78

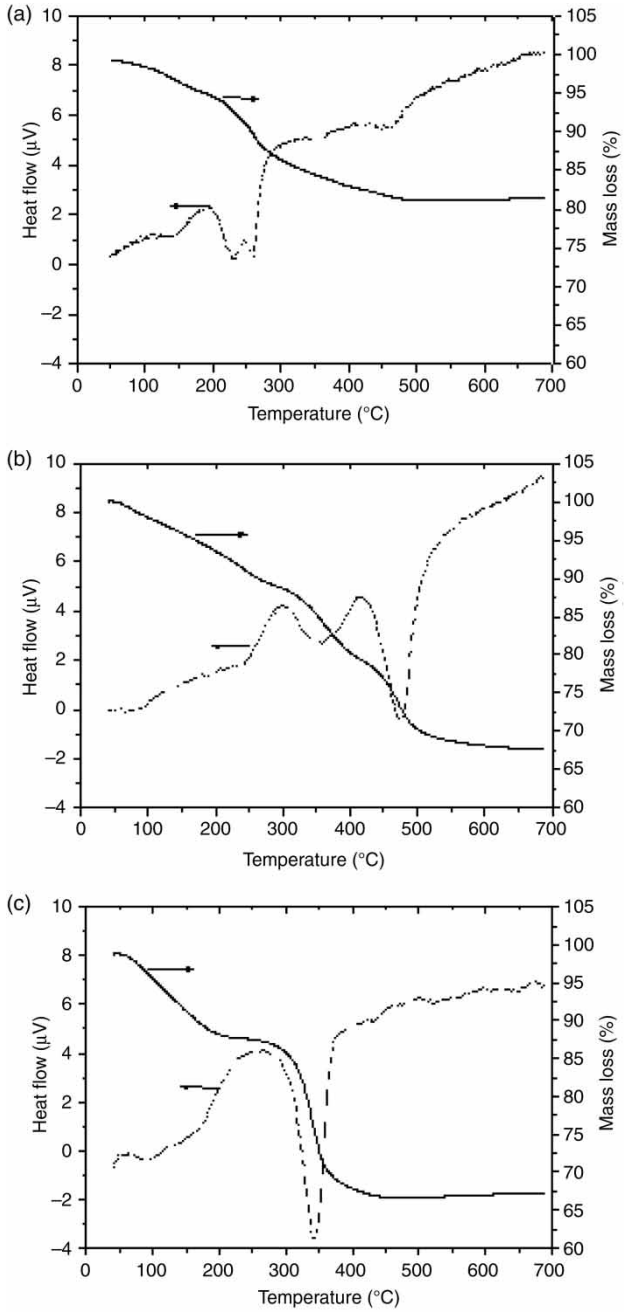

Figure 2 | TGA-DTA curves of Zn-Al-Cl (a), Mg-Al-Cl (b) and Ni-Al-Cl (c).

Downloaded from http://iwaponline.com/jwrd/article-pdf/7/3/307/376152/jwrd0070307.pdf
by guest

The third decomposition stage occurred in the range of 250–550°C with weight losses of approximately 9.65, 22.60 and 21.80%, for Zn-Al-Cl, Mg-Al-Cl and Ni-Al-Cl, respectively. These steps were assigned to the dehydroxylation of the inorganic layers in the LDH structure, decomposition of CO_3^{2-} anions impurities expected most likely to be due to the sorption and dissolution of carbon dioxide into the solution during the synthesis procedure and finally the elimination of chloride anions in the elevated temperature range. Dehydroxylation results in the collapse of the LDH structure and that of its corresponding metal oxides including MgO, NiO, ZnO, Al_2O_3 and $Mg/Zn/NiAl_2O_4$ at temperatures over 700°C (Malherbe & Pierre 2000; Palmer *et al.* 2009).

The TGA-DTA data show that the total mass loss for the Zn-Al-Cl, Mg-Al-Cl and Ni-Al-Cl are, respectively, 19.01, 33.32 and 34.30%. The temperature for decomposition of interlayer anions step decreases as the radii of M^{2+} ions increase. The presence of more M^{2+} cations in the LDHs shows in more positive charges on the brucite layers. This leads to stronger bonding between the layer structure and the chloride anions creating more stable LDH phases (Wang & Gao 2006). As more heat is required to decompose the LDHs, a higher temperature is necessary.

FTIR

FTIR spectra for all the LDHs shown in Figure 3 are characteristic for the hydrotalcite-like structures. The intense bands at approximately 3,558 cm^{-1} corresponded to the asymmetric and symmetric stretching mode vibration of OH groups in the layers (M/Al–OH or Al–OH) and the H_2O interlayer water molecules (Lakraimi *et al.* 2006). The small shoulder at 3,050 cm^{-1} corresponded to hydroxyl interactions with the impurities phase in the interlayer structure (Özgümüş *et al.* 2013). A weak absorption band at 1,630 cm^{-1} was related to the H_2O deformation bending (Elgaini *et al.* 2009). The sharp absorption band at 1,380 cm^{-1} and the small shoulder and weak band at 615 cm^{-1} were assigned, respectively, to unidentate carbonate symmetric stretching vibrations (O–C–O bond) for the LDH with CO_3^{2-} anions included into the interlayer (Wang & Gao 2006). A series of bands in the range of 1,000–400 cm^{-1} corresponded to the existence of lattice

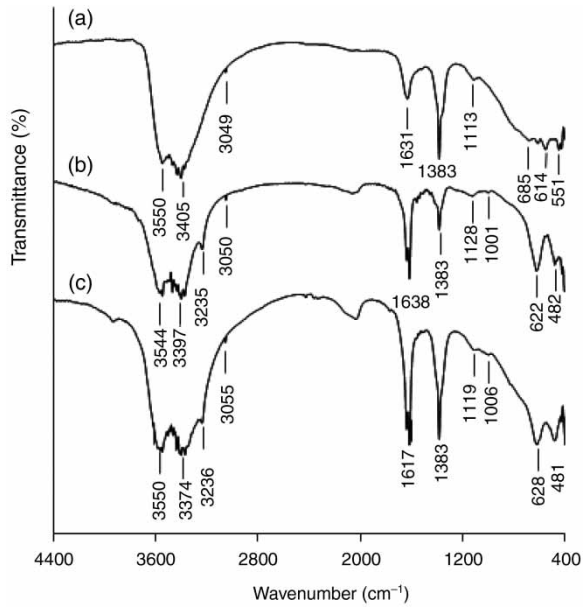

Figure 3 | FTIR spectra of (a) Zn-Al-Cl, (b) Mg-Al-Cl and (c) Ni-Al-Cl.

translational modes (Al–OH) or the carbonate bands (680 cm^{-1}) and vibrational modes of the lattice showing the $Al–O/M^{2+}–O/O–Al–O/O–M^{2+}–O$ bonds (448 cm^{-1}, 480 and 651 cm^{-1}) (Özgümüş *et al.* 2013). Other weak vibration bands or shoulders observed at 427 and 551 cm^{-1} corresponded to the $[AlO_6]^{3-}$ condensed groups vibrations, Mg/Al–OH translation, Al–OH translation, Al–OH deformation, $AlCl_4^-$ (400–580 cm^{-1}), Al_2Cl_6 (420–625 cm^{-1}) or metal–Cl such as Al–Cl/Mg–Cl stretching vibrations (at 625–400 cm^{-1} region) (Socrates 2001; Chen *et al.* 2010).

TEM observation

The surface morphology plays an important role in the adsorption properties of the LDH. Figure 4 shows the TEM images of synthesized LDHs. As can be seen, Zn-Al-Cl shows the platelet particles confirming the lamellar structure that was obtained by XRD analysis, and the particle size distribution was in the range from 50 to 150 nm. For Mg-Al-Cl, the image displays hexagonal platelet-like particles, the darker lines indicate the presence of aggregate crystallites which were probably obtained from a dense agglomeration of LDH particles (Patzkó *et al.* 2005). In the case of Ni-Al-Cl, the image shows that flower-like porous structures

Downloaded from http://iwaponline.com/jwrd/article-pdf/7/3/307/376152/jwrd0070307.pdf
by guest

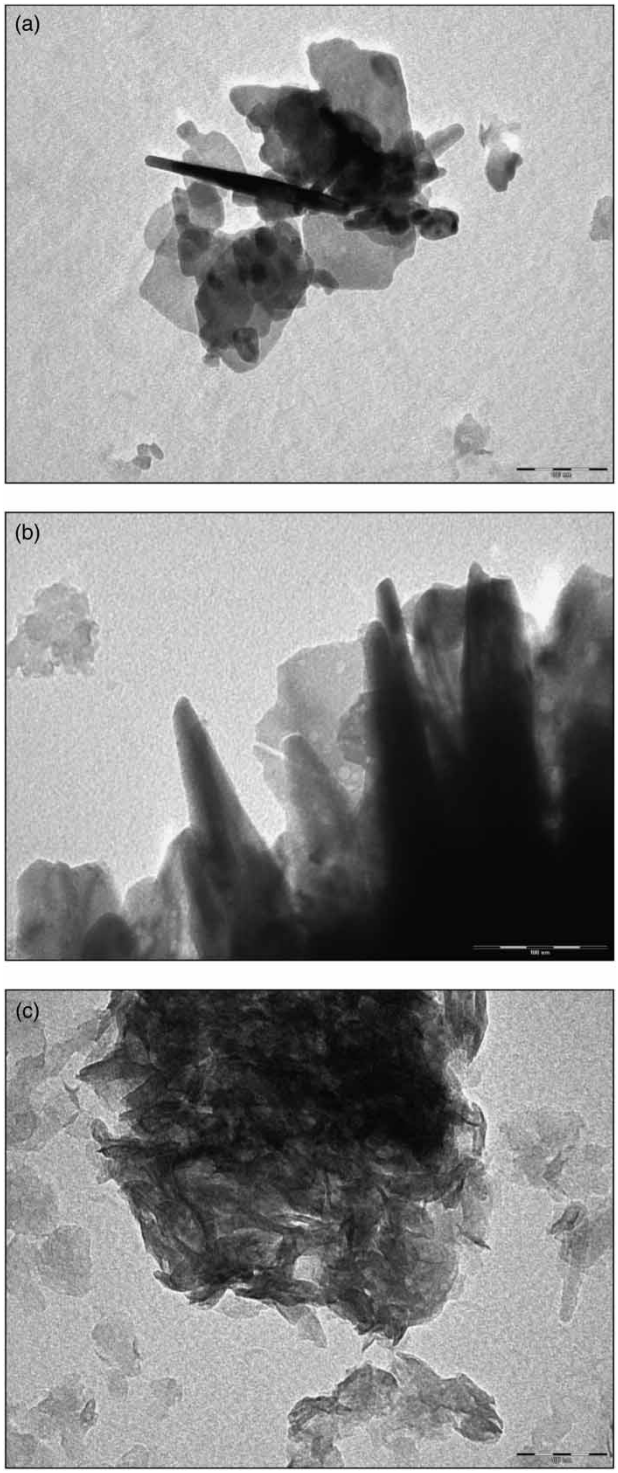

Figure 4 | TEM micrographs of the LDH samples: (a) Zn-AlCl, (b) Mg-AlCl and (c) Ni-AlCl.

were obtained. The observations confirm the high crystallinity of Zn-Al LDH and low crystallinity of Ni-Al LDH which were observed in the XRD patterns. This result can be explained by the presence of water and the nature of the interlayer in the structure.

Study of MO removal from aqueous solution

Effect of solution pH

The influence of solution pH on the MO removal by the materials was examined by the variation of the pH from 2 to 12 (Figure 5). The figure displays that the dye uptake was highly influenced by the solution pH. Maximum adsorptions were obtained at pH values approximate to 4: 233 mg/g for Zn-Al-Cl, 202 mg/g for Mg-Al-Cl and 186 mg/g for Ni-Al-Cl. In the interval of pH between 4 and 10, the removal quantity decreased with increasing solution pH. In addition, dye removal decreased when the pH value decreased below 4. Different parameters like adsorption capacity, active surface sites and charges may be ascribed to the adsorption behavior of the LDHs at different pHs. The effect of solution pH on dye adsorption can be explained by effects of the PZC of the materials and the pKa of the MO. The points of zero charge of the LDHs were 7.29, 7.36 and 7.12 for Zn-Al-Cl, Mg-Al-Cl and Ni-Al-Cl, respectively. The surface charge that results from the structure of LDHs can be modified by fixation of ions from the solution, such as H^+ or OH^- (Li *et al.* 2009). The surface of the samples was

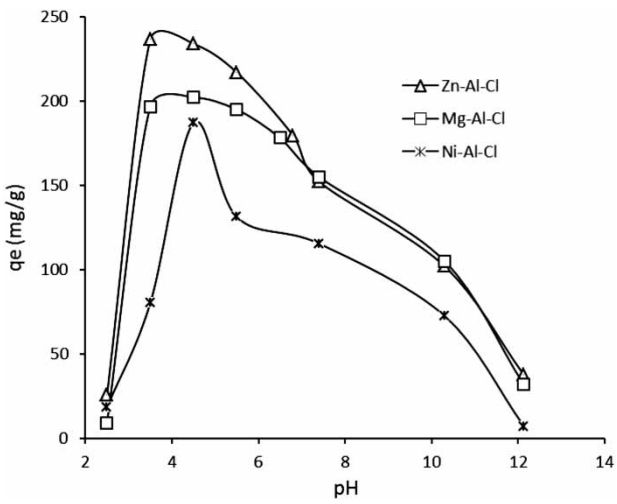

Figure 5 | Effect of solution pH on MO removal (adsorbent dose: 80 mg/L, contact time: 8 h, initial MO concentration: 20 mg/L, temperature: 25°C and agitation speed 500 rpm).

Downloaded from http://iwaponline.com/jwrd/article-pdf/7/3/307/376152/jwrd0070307.pdf
by guest

protonated and was charged positively when the pH value was below the PZC and deprotonated at pH values above the PZC.

At pH values lower than the PZC:

$$\text{Surface\_OH} + H_3O^+ \rightarrow \text{Surface} - OH_2^+ + H_2O$$

At pH values above the PZC:

$$\text{Surface\_OH} + OH^- \rightarrow \text{Surface} - O^- + H_2O$$

where Surface means the surface of the LDHs.

In the dissolution of the MO dye in the aqueous solution, the sulfonate groups of the dye (D – SO_3Na) are dissociated and transformed to:

$$D - SO_3Na \rightarrow D - SO_3^- + Na^+$$

The dissociation constant pKa for MO is 3.46, so MO molecules were predominantly present as monovalent anions above this equilibrium pH (Zollinger 2001).

At pH values between the PZC of LDHs and the pKa of MO, two possible process for dye elimination onto LDHs may be produced: the first possibility is anionic exchange of Cl^- anions in the interlayer structure by dye anions D – SO_3^-, the second is adsorption by combination between the positively charged surface – OH_2^+ of LDHs and anionic ions of MO dye D – SO_3^-. For pH values above the PZC, the positive charges on the surface of LDHs were reduced and the uptake of the dye also decreases. Moreover, the MO must be in concurrence with the hydroxyl group in the solution for exchange with the Cl^- anions. These cases explain the increase in the quantity adsorbed in acidic conditions. However, important diminution in dye removal below pH 4 can result from the destruction of the LDH structure, which was observed in other studies (Delgado *et al.* 2008).

Effect of contact time

Figure 6 exhibits the effect of contact time on the removal of MO by LDHs. The first observation indicates that the quantity of dye adsorbed increased rapidly within the first 60 min and then remained practically the same regardless of the concentration. The affinity of dye ions towards Zn-Al-Cl is more significant than that towards Mg-Al-Cl and Ni-Al-Cl. The rapid adsorption at the first contact time is due to the existence of a number of vacant sites on the surface of LDHs that are available for adsorption throughout the first step. The later slow rate is probably due to the anionic exchange between the dye and interlayer Cl^- anion.

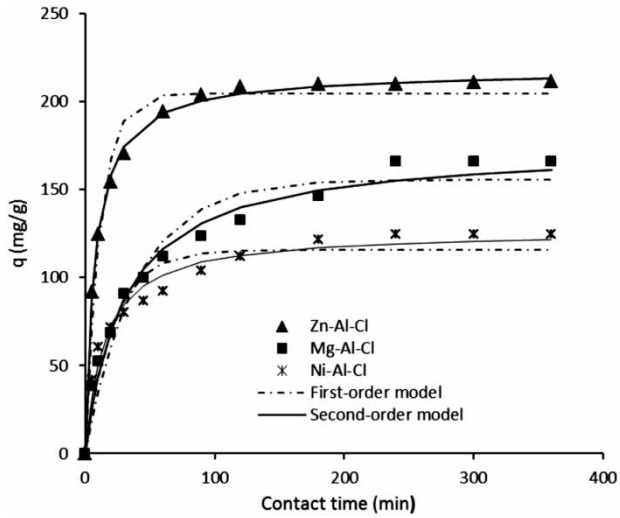

Figure 6 | Effect of contact time and kinetic models of MO adsorption (adsorbent dose: 80 mg/L, initial MO concentration: 20 mg/L, temperature: 25 °C, agitation speed 500 rpm and solution pH: 8).

In order to describe the kinetics involved in the process of adsorption, pseudo-first-order and pseudo-second-order rate equations were suggested and the kinetic data were examined founded on the regression coefficient (r^2) and the quantity of dye adsorbed per unit weight of the LDHs.

The first-order rate of Lagergren (1898) is founded on solid capacity and is generally shown as follows:

$$q = q_e(1 - e^{-k_1 t}) \tag{3}$$

where q_e and q (both in mg/g) are, respectively, the amounts of dye removed at equilibrium and at any time 't' and k_1 (1/min) is the rate constant of adsorption.

The pseudo-second-order model suggested by Ho & McKay (1999) is based on the hypothesis that the uptake follows second order chemisorption. This model can be expressed as:

$$q = \frac{k_2 q_e^2 t}{1 + k_2 q_e t} \tag{4}$$

Downloaded from http://iwaponline.com/jwrd/article-pdf/7/3/307/376152/jwrd0070307.pdf
by guest

where k_2 (g/mg.min) is the rate constant of pseudo-second-order adsorption.

The kinetic data determined for each model and the correlation coefficient (r^2) are shown in Table 2. As can be shown from the results, the two models exhibit a reasonably good agreement with the experimental data, but comparison between the r^2 values, indicates that the pseudo-second-order model gives the perfect overall fit. Furthermore, the adsorbed amounts at equilibrium calculated ($q_{e,cal}$) by this model are also a good fit with the experimental values ($q_{e,exp}$). The good fit with experimental data for all samples confirm that the velocity control mechanism of adsorption is chemical adsorption. Similar results for chemical adsorption of removal of dye contaminants onto LDHs were found by Zhu *et al.* (2005).

Adsorption isotherms

Figure 7 shows the isotherms of MO adsorption by Zn-Al-Cl, Mg-Al-Cl and Ni-Al-Cl. The figure indicates that, the equilibrium adsorption amounts increased with increasing equilibrium concentration. This result for adsorption amounts with concentration is maybe due to a greater driving force for mass transfer. In particular, high initial concentration in solution implies a high number of MO molecules fixed at the surface of the LDH. The isotherms shape was type L in Giles classification (1960). These types of isotherms are generally joined with ionic solute adsorption with weak competition with the solvent molecules. To better understand the adsorption process, the obtained equilibrium data were examined by different isotherm models. An isotherm is represented by some constants, the values of which show the surface properties and affinity of the adsorbent. Also, this can be used to determine the adsorption capacity of adsorbents. In this work, two well-known models of Langmuir (1916) and Freundlich & Heller (1939) were examined. The Langmuir model assumes that the number of surface sites are fixed, adsorption behavior is independent of surface coverage and all adsorption sites are similar. Therefore, the Langmuir isotherm model was selected for the evaluation of the maximum adsorption capacity (q_m) correlated to the complete monolayer coverage of the sorbent surface. The equation is given as:

$$q_e = \frac{q_m K_L C_e}{1 + K_L C_e} \tag{5}$$

where q_m (mg/g) is the maximum amount of MO fixed per unit mass of adsorbent and K_L (L/mg) is the Langmuir constant related to adsorbent/adsorbate affinity. C_e is the equilibrium concentration.

The Freundlich model isotherm represents an empirical equation that presumes that the adsorption surface is heterogeneous for the course of the adsorption process. The Freundlich isotherm is defined by the following equation:

$$q_e = K_F C_e^{\frac{1}{n}} \tag{6}$$

where K_F represents a value for the system, associated to the bonding energy, it can be motioned as the adsorption or distribution coefficient and indicates the quantity of dye adsorbed or fixed onto adsorbent for unit equilibrium concentration. $1/n$ represents the adsorption intensity of the dye molecules onto the sorbent or surface heterogeneity, which becomes more heterogeneous when the $1/n$ value becomes proximate to zero. A value for $1/n$ below 1 represents a normal Langmuir isotherm, while $1/n$ above 1 indicates a cooperative adsorption.

Table 2 | Pseudo-first-order model and pseudo-second-order model parameters for MO adsorption by LDHs

		Pseudo-first-order model			Pseudo-second-order model		
Adsorbent	q_{exp} (mg/g)	$q_{e,\,cal}$ (mg/g)	k_1 (1/min)	r^2	$q_{e,\,cal}$ (mg/g)	k_2 (g/mg·min)	r^2
Zn-Al-Cl	211.55	204.63	0.0859	0.973	217.36	0.00062	0.998
Mg-Al-Cl	166.23	155.78	0.0249	0.949	174.89	0.00019	0.985
Ni-Al-Cl	124.68	115.64	0.0460	0.910	126.57	0.00054	0.972

Downloaded from http://iwaponline.com/jwrd/article-pdf/7/3/307/376152/jwrd0070307.pdf
by guest

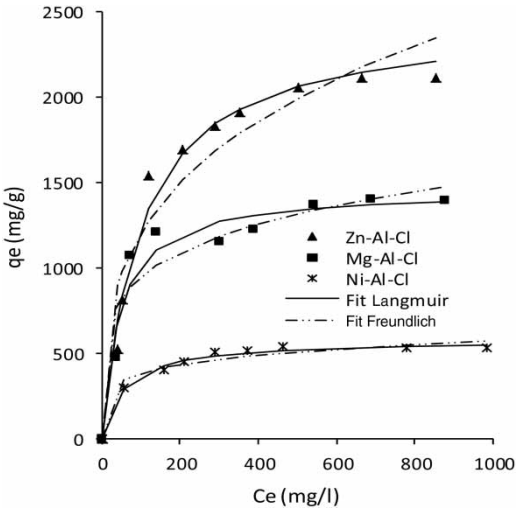

Figure 7 | Adsorption isotherms of MO onto LDHs (adsorbent dose: 80 mg/L, pH: 8, contact time: 8 h, temperature: 25 °C and agitation speed: 500 rpm).

The calculated isotherm parameters for each model and the correlation coefficients estimated by the nonlinear regressive process are summarized in Table 3. The table shows that the best fit of experimental data was obtained with the Langmuir model. The maximum Langmuir monolayer adsorption capacities were 2,758, 1,622 and 800 mg/g, respectively, for Zn-Al-Cl, Mg-Al-Cl and Ni-Al-Cl. This result was in agreement with XRD analysis, which demonstrated that Zn-Al-Cl presents a high interlayer distance.

Treatment of textile effluent

Tests were carried out on industrial wastes from a dyeing factory that used different dyes and chemical substances such as dispersants, detergents and salts. Their quantities in effluents vary in different production processes. Initial characterization of the effluent showed various physico-chemical parameters (Table 4). The pH of the sample

Table 3 | Isotherm constants for MO adsorption by LDHs

	Langmuir model			Freundlich model		
Adsorbent	q_m (mg/g)	K_L (L/mg)	r^2	K_F (mg/g) (L/mg)$^{1/n}$	n	r^2
Zn-Al-Cl	2,455.31	0.0103	0.985	295.75	3.260	0.926
Mg-Al-Cl	1,456.55	0.0225	0.951	371.59	4.918	0.909
Ni-Al-Cl	574.34	0.0180	0.992	169.97	5.698	0.962

Table 4 | Physico-chemical analysis of TWW

Parameters	Unit	Value	Moroccan standard
pH	–	8.9	5.5–9.0
Temperature	°C	30	30
COD	mg/L	614.6	250
Suspended solids	mg/L	23	150

effluent was observed as basic (8.9) and the temperature value was 30°C. It was also observed that the COD value (614.6 mg/L) was higher compared to the standard value.

For the verification of the capacity of LDHs to treat the effluent, the effect of the variation of adsorbents dose and pH on the percentage of decolorization and COD removal

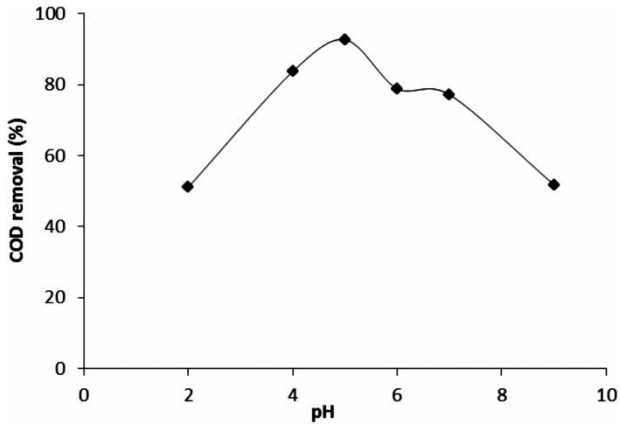

Figure 8 | Effect of pH on COD removal by Zn-Al-Cl (V = 20 mL, Agitation speed: 500 rpm, contact time: 8 h and adsorbent dose: 1 g/L).

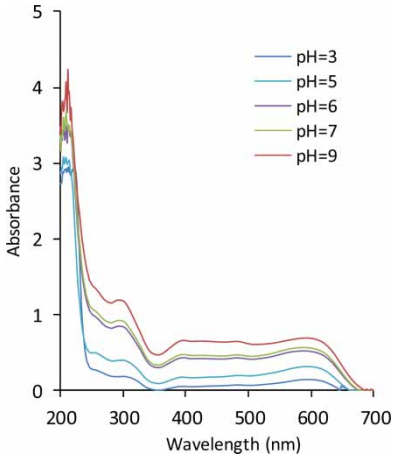

Figure 9 | Variation in UV-Vis spectra of TWW treated by Zn-Al-Cl at different pH solution (V = 20 ml. Agitation speed: 500 rpm, contact time: 8 h, adsorbent dose: 1 g/L).

Downloaded from http://iwaponline.com/jwrd/article-pdf/7/3/307/376152/jwrd0070307.pdf
by guest

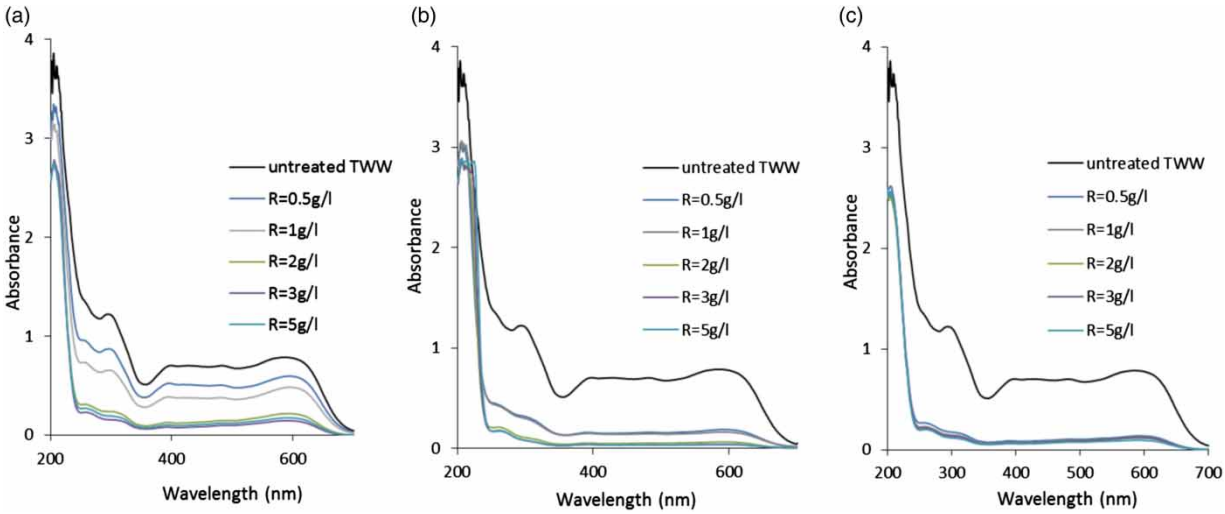

Figure 10 | Variation in UV-Visible spectra of TWW at different LDH dosages: (a) Zn-Al-Cl, (b) Mg-Al-Cl and (c) Ni-Al-Cl (pH = 5, V = 20 mL and contact time: 8 h).

from industrial textile effluent were investigated. Figure 8 shows the effect of pH on COD removal. The optimum pH was observed in the range of 4–7. The maximum COD removal was shown to be 92.95% at the pH value of 5. On the other hand, Figure 9 represents the evolution of the UV-Vis spectra of the TWW treated by Zn-Al-Cl at different solution pH values. The results show that the decolorization of TWW was obtained at pH of 5 and 6. So these results can be explained by pH_{PZC} and stability of LDHs which is reported and observed in the effect of pH on MO adsorption.

The effect of adsorbent dosage on the decolorization of TWW on the three adsorbents is presented by the UV-Vis spectrum in Figure 10. This figure indicates that the decrease of the absorbance is associated with the increase in adsorbent dosage. These results are explained by a reduction of chromophore groups which is responsible for colorization of textile effluent. A rapid decrease in the absorbance of TWW was observed and 90% of the color was removed at 5 g/L for Zn-Al-Cl and there was a great capacity of decolorization at low adsorbent dose for Mg-Al-Cl and Ni-Al-Cl. These results suggest that the precursors present a high capacity of decolorization of the textile effluent.

The effect of the LDH dose on COD removal for the three adsorbents was evaluated by the variation of the dose from 0.5 to 5 g/L. The results are given in Figure 11 and indicate that COD removal increases with increasing the quantity of adsorbent. The figure also shows that increasing the dose beyond 2 g/L had little effect on the COD

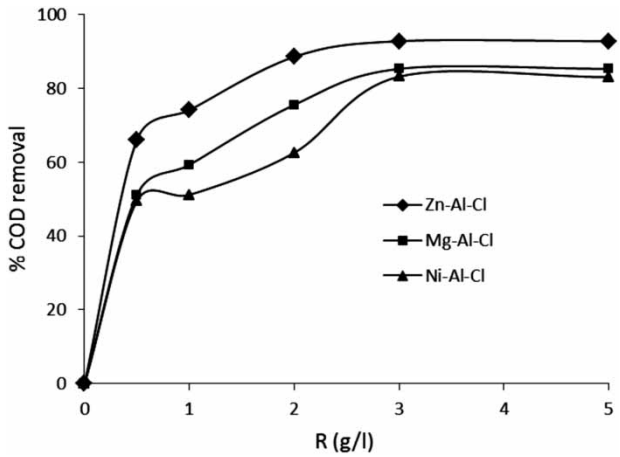

Figure 11 | Effect of adsorbent dosage on COD removal by LDHs (pH 5, V = 20 mL and contact time: 8 h).

reduction and hence this value was considered as the optimum. The maximum percentage of COD removed from the TWW is noted as 92.84% in the case of Zn-Al-Cl.

CONCLUSION

From the present study, it can be concluded that the M/Al-Cl LDHs (M = Zn, Mg, Ni) were successfully prepared by the co-precipitation method. The XRD patterns display high crystallinity of Zn-Al-Cl compared to Ni-Al-Cl and Mg-Al-Cl, and the interlayer distance was dependent on

Downloaded from http://iwaponline.com/jwrd/article-pdf/7/3/307/376152/jwrd0070307.pdf
by guest

the cation ionic radii. Experiments examined the decolorization of MO from aqueous solutions by LDHs, indicating that the MO could be adsorbed on Mg-Al-Cl, Zn-Al-Cl and Ni-Al-Cl LDHs. The results indicated that the pH influences the surface charge of the precursors and the quality of acid dye dissociation. The effective pH range for MO removal was obtained at pH values approximate to 4. Equilibrium uptake was increased by increasing the initial dye concentration. The adsorption isotherm of dye by LDHs could be well fitted by the Langmuir model with a high adsorption capacity equal to 2,455.31 mg/g for Zn-Al-Cl. The high adsorption capacity of LDHs in this study indicates that they are a promising precursor for the treatment of actual dye by the decolorization and COD uptake from TWW. The maximum percentage of COD removed from the TWW is noted as 92.84% in the case of Zn-Al-Cl.

REFERENCES

American Public Health Association 1998 *Standard Methods for the Examination of Water and Wastewater*, 20th edn. American Public Health Association/American Water Works Association/Water Environment Federation, Washington, DC, USA.

Barka, N., Assabbane, A., Nounah, A., Laanab, L. & Ichou, Y.A. 2009 Removal of textile dyes from aqueous solution by natural phosphate as new adsorbent. *Desalination* **235**, 264–275.

Carlino, S. 1997 The intercalation of carboxylic acids into layered double hydroxides: a critical evaluation and review of the different methods. *Solid State Ionics* **98**, 73–84.

Cavani, F., Trifiro, F. & Vaccari, A. 1991 Hydrotalcite-type anionic clays: preparation, properties and applications. *Catalysis Today* **11**, 173–301.

Chen, Y., Lia, F., Zhoua, S., Weia, J., Daia, Y. & Chen, Y. 2010 Structure and photoluminescence of Mg–Al–Eu ternary hydrotalcite-like layered double hydroxides. *Journal of Solid State Chemistry* **183**, 2222–2226.

Crini, G. 2006 Non-conventional low-cost adsorbents for dye removal: a review. *Bioresource Technology* **97**, 1061–1085.

Dawood, S. & Sen, T. K. 2012 Removal of anionic dye Congo red from aqueous solution by raw pine and acid-treated pine cone powder as adsorbent: equilibrium, thermodynamic, kinetics, mechanism and process design. *Water Research* **46**, 1933–1946.

Delgado, R. R., De Pauli, C. P., Carrasco, C. B. & Avena, M. J. 2008 Influence of MII/MIII ratio in surface-charging behavior of Zn–Al layered double hydroxides. *Applied Clay Science* **40**, 27–37.

Demirbas, A. 2009 Agricultural based activated carbons for the removal of dyes from aqueous solutions: a review. *Journal of Hazardous Materials* **167**, 1–9.

Dotto, G. L. & Pinto, L. A. A. 2011 Adsorption of food dyes acid blue 9 and food yellow 3 onto chitosan: stirring rate effect in kinetics and mechanism. *Journal of Hazardous Materials* **187**, 164–170.

Elgaini, L., Lakraimi, M., Sebbar, E., Meghea, A. & Bakasse, M. 2009 Removal of indigo carmine dye from water to Mg–Al–CO_3-calcined layered double hydroxides. *Journal of Hazardous Materials* **161**, 627–632.

Elmoubarki, R., Mahjoubi, F. Z., Tounsadi, H., Moustadraf, J., Abdennouri, M., Zouhri, A., ElAlbani, A. & Barka, N. 2015 Adsorption of textile dyes on raw and decanted Moroccan clays: kinetics, equilibrium and thermodynamics. *Water Resources and Industry* **9**, 16–29.

Freundlich, H. & Heller, W. 1939 The adsorption of cis- and trans-azobenzene. *Journal of American Chemical Society* **61**, 2228–2230.

Giles, C. H., MacEwan, T. H., Nakhwa, A. N. & Smith, D. 1960 Studies in adsorption. Part XI. A system of classification of solution adsorption isotherms and its use in diagnosis of adsorption mechanisms and in measurement specific surface of solids. *Journal of Chemical Society* **111**, 3973–3993.

GuptaV. K. & Suhas 2009 Application of low-cost adsorbents for dye removal – a review. *Journal of Environmental Management* **90**, 2313–2342.

Ho, Y. S. & Mckay, G. 1999 Pseudo-second order model for sorption processes. *Process Biochemistry* **34**, 451–465.

Lagergren, S. 1898 About the theory of so-called adsorption of soluble substance Seven Vetenskapsakad. *Handband* **24**, 1–39.

Lakraimi, M., Legrouri, A., Barroug, A., De Roy, A. & Besse, J. P. 2006 Synthesis and characterisation of a new stable organo-mineral hybrid nanomaterial: 4-chlorobenzenesulfonate in the zinc-aluminium layered double hydroxide. *Materials Research Bulletin* **41**, 1763–1774.

Langmuir, I. 1916 The constitution and fundamental properties of solids and liquids. *Journal of American Chemical Society* **38**, 2221–2295.

Li, F., Wang, Y., Yang, Q., Evans, D. G., Forano, C. & Duan, X. 2005 Study on adsorption of glyphosate (*N*-phosphonomethyl glycine) pesticide on MgAl-layered double hydroxides in aqueous solution. *Journal of Hazardous Materials* **125**, 89–95.

Li, Y., Gao, B., Wu, T., Wang, B. & Li, X. 2009 Adsorption properties of aluminum magnesium mixed hydroxide for the model anionic dye Reactive Brilliant Red K-2BP. *Journal of Hazardous Materials* **164**, 1098–1104.

Lopez-Salinas, E. & Ono, Y. 1993 Intercalation chemistry of a Mg-Al layered double hydroxides ion-exchanged with complex MCl_4^{2-} (M = Ni, Co) ions from organic media. *Microporous Materials* **1**, 33–42.

Malherbe, F. & Pierre, B. J. 2000 Investigating the effects of guest-host interactions on the properties of anion-exchanged Mg–Al hydrotalcites. *Journal of Solid State Chemistry* **155**, 332–341.

Noh, J. S. & Schwarz, J. A. 1989 Estimation of the point of zero charge of simple oxides by mass titration. *Journal of Colloid Interface Science* **130**, 157–164.

Özgümüş, S., Gök, M. K., Bal, A. & Güçlü, G. 2013 Study on novel exfoliated polyampholyte nanocomposite hydrogels based on

Downloaded from http://iwaponline.com/jwrd/article-pdf/7/3/307/376152/jwrd0070307.pdf
by guest

acrylic monomers and Mg-Al-Cl layered double hydroxide: synthesis and characterization. *Chemical Engineering Journal* **223**, 277–286.

Palmer, S. J., Ray, L. & Nguyen, T. 2009 Hydrotalcites and their role in coordination of anions in Bayer liquors: anion binding in layered double hydroxides. *Coordination Chemistry Reviews* **253**, 250–267.

Patzkó, A., Kun, R., Hornok, V., Dékány, I., Engelhardt, T. & Schall, N. 2005 ZnAl-layer double hydroxides as photocatalysts for oxidation of phenol in aqueous solution. *Colloids and Surfaces A* **265**, 64–72.

Rafatullaha, M., Sulaimana, O., Hashima, R. & Ahmad, A. 2010 Adsorption of methylene blue on low-cost adsorbents: a review. *Journal of Hazardous Materials* **177**, 70–80.

Saleh, T. A. & Gupta, V. K. 2012 Photo-catalyzed degradation of hazardous dye methyl orange by use of a composite catalyst consisting of multi-walled carbon nanotubes and titanium dioxide. *Journal of Colloid and Interface Science* **371**, 101–106.

Santhy, K. & Selvapathy, P. 2006 Removal of reactive dyes from wastewater by adsorption on coir pith activated carbon. *Bioresource Technology* **97**, 1329–1336.

Shannon, R. D. 1976 Revised effective ionic radii and systematic studies of interatomic distances in halides and chalcogenides. *Acta Crystallographica* **32**, 751–767.

Shen, D., Fan, J., Zhou, W., Gao, B., Yue, Q. & Kang, Q. 2009 Adsorption kinetics and isotherm of anionic dyes onto organo-bentonite from single and multisolute systems. *Journal of Hazardous Materials* **172**, 99–107.

Socrates, G. 2001 *Infrared and Raman Characteristic Group Frequencies*, 3rd edn. John Wiley & Sons, New York.

Tounsadi, H., Khalidi, A., Abdennouri, M. & Barka, N. 2016 Potential capability of natural biosorbents: *Diplotaxis harra* and *Glebionis coronaria* L. on the removal efficiency of dyes from aqueous solutions. *Desalination and Water Treatment* **57** (35), 16633–16642.

Vanderborght, M. & Van Grieken, E. 1977 Enrichment of trace metals in water by adsorption on activated carbon. *Analytical Chemistry* **49**, 311–316.

Wang, Y. & Gao, H. 2006 Compositional and structural control on anion sorption capability of layered double hydroxides (LDHs). *Journal of Colloid and Interface Science* **301**, 19–26.

Whilton, N. T. P., Vickers, J. & Mann, S. 1997 Bioinorganic clays: synthesis and characterization of amino- and polyamine acid intercalated layered double hydroxides. *Journal of Materials Chemistry* **7**, 1623–1629.

Zhu, M. X., Li, Y. P., Xie, M. & Xin, H. Z. 2005 Sorption of an anionic dye by uncalcined and calcined layered double hydroxides: a case study. *Journal of Hazardous Materials* **120**, 163–171.

Zhu, M.-X., Lee, L., Wang, H.-H. & Wang, Z. 2007 Removal of an anionic dye by adsorption/precipitation processes using alkaline white mud. *Journal of Hazardous Materials* **149**, 735–741.

Zollinger, H. 2001 *Color Chemistry: Syntheses, Properties, and Applications of Organic Dyes and Pigments*, 3rd edn. WILEY-VCH, Zurich.

First received 14 February 2016; accepted in revised form 23 April 2016. Available online 1 June 2016

Downloaded from http://iwaponline.com/jwrd/article-pdf/7/3/307/376152/jwrd0070307.pdf
by guest